

## Labeling strategies for $^{13}\text{C}$ -detected aligned-sample solid-state NMR of proteins

Fabian V. Filipp, Neeraj Sinha, Lena Jairam, Joel Bradley, Stanley J. Opella \*

Department of Chemistry and Biochemistry, University of California, San Diego, 9500 Gilman Drive, La Jolla, CA 92093-0307, USA  
Cambridge Isotope Laboratories, 50 Frontage Road, Andover, MA 01810, USA

### ARTICLE INFO

#### Article history:

Received 8 July 2009

Revised 26 August 2009

Available online 2 September 2009

#### Keywords:

$^{13}\text{C}$  labeling

PISEMA

Solid-state NMR

Tailored isotopic labeling

Triple resonance

### ABSTRACT

$^{13}\text{C}$ -detected solid-state NMR experiments have substantially higher sensitivity than the corresponding  $^{15}\text{N}$ -detected experiments on stationary, aligned samples of isotopically labeled proteins. Several methods for tailoring the isotopic labeling are described that result in spatially isolated  $^{13}\text{C}$  sites so that dipole–dipole couplings among the  $^{13}\text{C}$  are minimized, thus eliminating the need for homonuclear  $^{13}\text{C}$ – $^{13}\text{C}$  decoupling in either indirect or direct dimensions of one- or multi-dimensional NMR experiments that employ  $^{13}\text{C}$  detection. The optimal percentage for random fractional  $^{13}\text{C}$  labeling is between 25% and 35%. Specifically labeled glycerol and glucose can be used at the carbon sources to tailor the isotopic labeling, and the choice depends on the resonances of interest for a particular study. For investigations of the protein backbone, growth of the bacteria on [2- $^{13}\text{C}$ ]-glucose-containing media was found to be most effective.

© 2009 Elsevier Inc. All rights reserved.

### 1. Introduction

The majority of aligned-sample solid-state NMR studies on proteins immobilized in supramolecular complexes, such as virus particles or membranes, have relied on  $^1\text{H}/^{15}\text{N}$  double-resonance experiments [1]. There are several advantages to this approach, including the relative ease and low cost of labeling all nitrogen sites in proteins obtained by expression in bacteria [2]. Solid-state NMR experiments on uniformly  $^{15}\text{N}$  labeled proteins are straightforward because they have no nitrogen atoms directly bonded to other nitrogen atoms in either backbone or side chain sites. As a result, there is no need to implement homonuclear  $^{15}\text{N}$  decoupling at any stage in the pulse sequences, including during the direct acquisition of  $^{15}\text{N}$  signals, and the requisite heteronuclear decoupling is accomplished by irradiation of the  $^1\text{H}$  resonances. It is feasible to make accurate measurements of  $^1\text{H}$  chemical shift,  $^{15}\text{N}$  chemical shift, and  $^1\text{H}$ – $^{15}\text{N}$  heteronuclear dipolar coupling frequencies for individual sites, as well as to detect  $^1\text{H}$ – $^1\text{H}$  and weak  $^{15}\text{N}$ – $^{15}\text{N}$  homonuclear couplings using a wide variety of multi-dimensional NMR experiments.

However, there are two disadvantages to the  $^1\text{H}/^{15}\text{N}$  double-resonance approach: it is restricted to the amide nitrogen sites in the polypeptide backbone and the few nitrogen-containing side chain sites, and the direct detection of  $^{15}\text{N}$  signals has low sensitivity because of its low gyromagnetic ratio. Both of these issues can

be addressed by implementing  $^1\text{H}/^{13}\text{C}/^{15}\text{N}$  triple-resonance experiments on proteins labeled with both  $^{13}\text{C}$  and  $^{15}\text{N}$ . The sensitivity can be improved by detecting  $^{13}\text{C}$  signals because its gyromagnetic ratio is about 2.5 times larger than that of  $^{15}\text{N}$ , and there is the opportunity to obtain spectroscopic data from nearly all backbone and side chain sites. The design of triple-resonance experiments for stationary samples is considerably different than that for magic angle spinning (MAS) experiments. In this article, we describe progress towards the development of isotopic labeling schemes compatible with direct detection of  $^{13}\text{C}$  signals in  $^1\text{H}/^{13}\text{C}/^{15}\text{N}$  triple-resonance experiments on stationary aligned samples [3–10] by examining a wide range of  $^{13}\text{C}$  labeling approaches [11] over an array of fractions of dilutions, ranging from 15% to 100% of all sites in the proteins, and [2- $^{13}\text{C}$ ]-glucose in addition to the complementarily labeled glycerols for labeling through metabolic pathways. Magnetically aligned filamentous bacteriophage particles are used as the samples to demonstrate the influence of the labeling patterns on solid-state NMR spectra.

In single-contact spin-lock cross-polarization experiments on single crystals of peptides and aligned samples of proteins, we have observed a fourfold improvement in the signal-to-noise ratio when  $^{13}\text{C}$  magnetization is detected compared to  $^{15}\text{N}$  magnetization for individual labeled sites in the same samples under equivalent experimental conditions [7]. As is the case for  $^{15}\text{N}$  labeling of proteins expressed in bacteria, 100% uniform labeling of all carbon sites with  $^{13}\text{C}$  is straightforward when completely labeled carbon sources, such as  $^{13}\text{C}_6$  glucose or  $^{13}\text{C}_3$  glycerol, are used in the growth media. However, in protein samples where all of the carbon sites are labeled with  $^{13}\text{C}$ , the homonuclear dipole–dipole couplings among the dense network of bonded and nearby  $^{13}\text{C}$  nuclei

\* Corresponding author. Address: Department of Chemistry and Biochemistry, University of California, San Diego, 9500 Gilman Drive, Natural Sciences Building, Rm. 3119, La Jolla, CA 92093-0307, USA. Fax: +1 858 822 4821.

E-mail address: [sopella@ucsd.edu](mailto:sopella@ucsd.edu) (S.J. Opella).

present significant complications in solid-state NMR of stationary samples. Indeed, one of the principal advantages of high-speed magic angle spinning solid-state NMR experiments is that the homonuclear dipole–dipole couplings among the  $^{13}\text{C}$  sites are greatly attenuated. In contrast, in stationary samples, the  $^{13}\text{C}$  homonuclear couplings must be dealt with in order to obtain high-resolution spectra and to realize the sensitivity advantages of  $^{13}\text{C}$  detection.

There are two approaches to dealing with the homonuclear  $^{13}\text{C}$ – $^{13}\text{C}$  dipole–dipole couplings in stationary aligned samples. The first is to apply multiple-pulse homonuclear decoupling sequences to the  $^{13}\text{C}$  nuclei [12]. We have demonstrated the efficacy of this approach in the indirect dimensions of multi-dimensional experiments that enable  $^{13}\text{C}$  chemical shift frequencies to be measured; however, these experiments were performed with  $^{15}\text{N}$ -detection in the direct dimension [4]. The detection of signals in the windows of multiple-pulse sequences rarely leads to optimal sensitivity because of the filtering limitations associated with the short periods of time available for sampling the signals. The second approach is to tailor the pattern of isotopic labeling so that the  $^{13}\text{C}$  labeled sites of interest are sufficiently isolated from other  $^{13}\text{C}$  nuclei to eliminate the need for homonuclear decoupling.

The isotopic labeling schemes described in this article generate samples with spatially isolated  $^{13}\text{C}$  sites so that dipole–dipole couplings among the  $^{13}\text{C}$  are minimized, thus eliminating the need for homonuclear  $^{13}\text{C}$ – $^{13}\text{C}$  decoupling in either indirect or direct dimensions of one- or multi-dimensional NMR experiments that employ  $^{13}\text{C}$  detection. The isotopic precursors utilized for tailored labeling of proteins expressed in bacteria range from specifically labeled two-, three-, or six-carbon molecules to random fractionally labeled growth media prepared from algae grown in the presence of a defined mixtures of  $^{12}\text{C}$  and  $^{13}\text{C}$  carbon dioxide. The coupling among  $^{13}\text{C}$  nuclei is avoided either as a result of the alternate site pattern of metabolic incorporation [13–15] or because of the low statistical probability of two  $^{13}\text{C}$  nuclei being bonded to each other. Here, results from uniform  $^{13}\text{C}$  labeling and metabolically tailored  $^{13}\text{C}_\alpha$  labeling based on  $[2-^{13}\text{C}]$ -glucose,  $[2-^{13}\text{C}]$ -glycerol, or  $[1,3-^{13}\text{C}]$ -glycerol are compared to fractional  $^{13}\text{C}$  labeling. Two-dimensional projections of triple-resonance solution-state NMR spectra are used to characterize the labeling patterns. The filamentous bacteriophages fd, which infects *Escherichia coli*, and Pf1, which infects *Pseudomonas aeruginosa*, are used for the experimental demonstrations. The structural forms of the major coat proteins are immobilized and aligned along with the virus particles by the magnetic field for solid-state NMR experiments, and the membrane-bound forms of the same proteins are solubilized in detergent micelles for solution NMR experiments. The bacteriophage samples provide direct insights into the spectroscopic effects of the  $^{13}\text{C}$  labeling schemes at different protein backbone sites in solid-state NMR experiments. They have been used in complementary magic angle spinning studies [16,17].

## 2. Results

Filamentous bacteriophage samples were obtained from bacterial cultures grown on algal-based media containing various fractions of  $^{13}\text{C}$  labeled nutrients, or on minimal media supplemented with  $[2-^{13}\text{C}]$ -glucose,  $[2-^{13}\text{C}]$ -glycerol, or  $[1,3-^{13}\text{C}]$ -glycerol. In this article, our main focus is on the  $^1\text{H}$ – $^{13}\text{C}_\alpha$  sites that are uniformly distributed throughout the protein backbone, separated from each other by three bonds, and have one directly bonded hydrogen (except for glycine and proline). At the intersection of peptide planes, the associated  $^1\text{H}$  chemical shift,  $^{13}\text{C}$  chemical shift, and  $^1\text{H}$ – $^{13}\text{C}$  dipolar couplings provide valuable structural constraints, and enable direct comparisons of sensitivity and resolution between  $^{15}\text{N}$ - and  $^{13}\text{C}$ -detected experiments.

In the absence of homonuclear decoupling, only proteins labeled such that the  $^{13}\text{C}_\alpha$  sites are isotopically isolated from other  $^{13}\text{C}$ , i.e., bonded to  $^{12}\text{C}_\beta$  and  $^{12}\text{C}_\gamma$  (Fig. 1A), will yield solid-state NMR spectra with high resolution and sensitivity in stationary samples. The presence of  $^{13}\text{C}$  in either or both adjacent carbon sites (Fig. 1B) will result in broadened signals due to the presence of unresolved  $^{13}\text{C}$ – $^{13}\text{C}$  dipolar couplings. The probability of having an isolated  $^{13}\text{C}_\alpha$  site can be calculated from the individual probabilities of having  $^{13}\text{C}_\alpha$ ,  $^{12}\text{C}_\beta$ , and  $^{12}\text{C}_\gamma$  present in the same polypeptide with random  $^{13}\text{C}$  labeling at various fractions. As shown in Fig. 1D, the maximum probability occurs near a labeling ratio  $p = 1/3$ . Because the maximum is broad and both natural abundance  $^{13}\text{C}$  and the enrichment of  $^{13}\text{C}$  in other proximate sites are potential complications, we prepared custom algal media with  $^{13}\text{C}$  percentages of 15%, 25%, 35%, and 45%, as marked by arrows in Fig. 1D, in order to experimentally determine the optimal isotopic composition for solid-state NMR spectroscopy on stationary aligned samples of proteins.

The isotope labeling patterns of the protein samples were analyzed using solution NMR spectra. In general, the proteins were uniformly labeled to the predicted extent in all carbon sites in both *E. coli* and *P. aeruginosa* when grown on the algal-based media. One-dimensional  $^1\text{H}$ -decoupled,  $^{13}\text{C}$  solution NMR spectra report on the  $^{13}\text{C}$  labeling at all sites, including the carbonyl and aromatic ring carbons that are not directly bonded to hydrogens. However, only a detailed analysis of individual sites reveals whether labeled sites are isotopically isolated. Since *E. coli* is the host for fd bacteriophage, its major coat protein represents the labeling that occurs in this bacterium. Solution NMR spectra of the membrane-bound form of fd coat protein in micelles are shown in Fig. 2. The comparison of the spectrum obtained on a 25% uniformly labeled sample (Fig. 2A) and that from a sample labeled from media containing  $[2-^{13}\text{C}]$ -glucose (Fig. 2B) demonstrates that there is a greater extent of  $^{13}\text{C}$  labeling in the  $\text{C}_\alpha$  region (45–65 ppm) and reduced labeling in the aliphatic (0–50 ppm), aromatic (110–170 ppm), and carbonyl (165–185 ppm) regions in the  $[2-^{13}\text{C}]$ -glucose labeled sample.

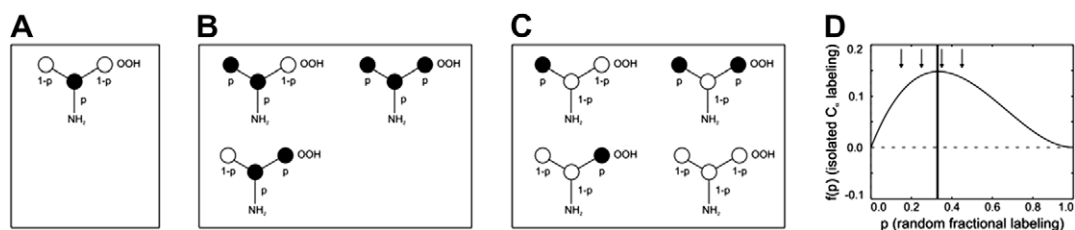


**Fig. 1.** Analysis of fractional uniform  $^{13}\text{C}$  labeling at the  $\text{C}_\alpha$  sites in the polypeptide backbone. (A) Schematic chemical structure of an isolated  $^{13}\text{C}_\alpha$  site bonded only to  $^{12}\text{C}$  that would contribute a high resolution NMR signal. (B) Schematic chemical structure of a non-isolated  $^{13}\text{C}_\alpha$  site bonded to  $^{13}\text{C}_\beta$  and/or  $^{13}\text{C}_\gamma$  sites that would contribute a broadened or undetectable NMR signal. (C) Schematic chemical structure of an unlabeled  $^{12}\text{C}_\alpha$  site that would not contribute a signal. (D) The probability ( $p$ ) of occurrence of an isolated  $^{13}\text{C}_\alpha$  sites that would contribute high resolution NMR signals is predicted by the function  $f(p) = p(1 - p)^2$ . The arrows denote the experimentally tested labeling ratios of 15%, 25%, 35%, and 45%.

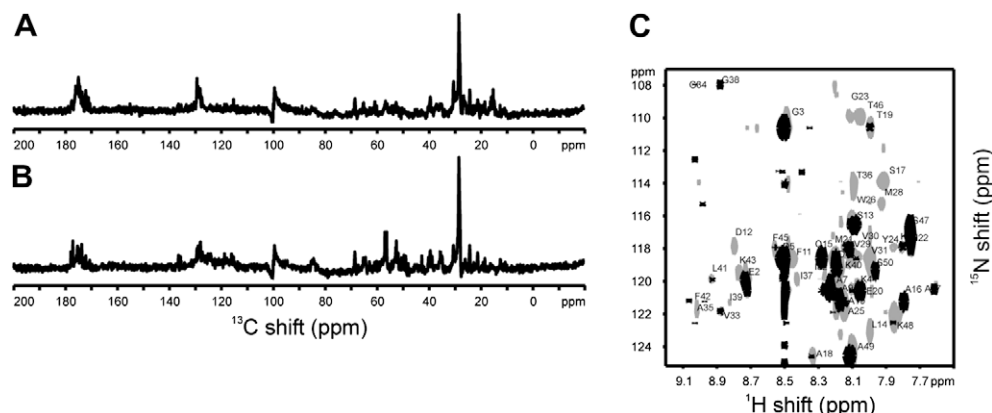


**Fig. 2.** Analysis of  $^{13}\text{C}$  labeling patterns of proteins obtained from *E. coli* by solution NMR of fd coat protein in micelles. (A and B) One-dimensional direct-detected  $^{13}\text{C}$  NMR spectra obtained by direct excitation. (A) The protein was obtained from bacteria grown on 25% uniformly  $^{13}\text{C}$  labeled media. (B) The protein was obtained from bacteria grown on  $[2-^{13}\text{C}]$ -glucose-containing media. (C) Overlay of two-dimensional  $^{13}\text{C}$ -edited  $^1\text{H}/^{15}\text{N}$  correlation spectra of the proteins whose spectra are shown in (A and B). Grey indicates 25% uniformly labeled with  $^{13}\text{C}$  and black indicates labeled by growth on  $[2-^{13}\text{C}]$ -glucose-containing media.

A combination of two-dimensional projections from three-dimensional heteronuclear solution NMR spectra is used to quantify the  $^{13}\text{C}$  enrichment at the  $\text{C}_\alpha$ ,  $\text{C}_\beta$ , and  $\text{C}_\gamma$  sites of the proteins. The choice of experiments utilized for this purpose depends on the availability of resonance assignments as well as which sites are of interest. The labeling at  $\text{C}_\alpha$  and  $\text{C}_\gamma$  sites can be assessed by comparison of peak intensities in  $^{13}\text{C}$ -edited  $^1\text{H}/^{15}\text{N}$  correlation spectra of the various  $^{13}\text{C}$  labeled samples at equal concentrations, and this requires only backbone amide proton assignments (Figs. 2C and 3). If  $^1\text{H}$ ,  $^{13}\text{C}$  assignments are available,  $^1\text{H}/^{13}\text{C}$  correlation spectra, e.g., two-dimensional  $^1\text{H}/^{13}\text{C}$  HMQC or  $^1\text{H}/^{13}\text{C}$  projections of three-dimensional HNCA, HNCB, and HNCOC spectra can be used to elucidate the  $^{13}\text{C}$  labeling of the protein. The  $^{13}\text{C}$  labeling results for *E. coli* grown on  $[2-^{13}\text{C}]$ -glucose-containing media are summarized in Fig. 4 for the  $\text{C}_\alpha$  and  $\text{C}_\gamma$  sites of fd coat protein.  $^{13}\text{C}$  is enriched in the  $\text{C}_\alpha$  sites of all residues to a level that is  $>18\%$ , except for leucine, and some approach 70%. The data summarized in Fig. 4B shows that the  $\text{C}_\gamma$  sites of isoleucine, leucine, proline, threonine, and tyrosine have enrichment levels  $>18\%$ , but that most amino acids undergo minimal labeling of their  $\text{C}_\gamma$  sites.

The coat protein of Pf1 bacteriophage reflects the metabolic pathways of its host organism *P. aeruginosa*, which are known to differ from those of *E. coli* [16,17]. The labeling patterns of proteins from *P. aeruginosa* were assessed using the same solution NMR approach used for *E. coli*. All of the proteins are 100% uniformly labeled with  $^{15}\text{N}$  in all nitrogen sites, and this provides a spectroscopic reference for the  $^{13}\text{C}$  resonance intensities. Column A in Fig. 5 contains the  $^{15}\text{N}$ -edited  $^1\text{H}$  NMR spectra of all of the samples of the membrane-bound form of Pf1 coat protein in micelles that are directly comparable to the  $^{13}\text{C}$  NMR spectra in Column B. The corresponding one-dimensional solid-state  $^{13}\text{C}$  NMR spectra of the structural form of Pf1 coat protein in magnetically aligned bacteriophage particles are shown in Column C; these spectra are analyzed in three regions, with the broad band of resonances near 200 ppm from the carbonyl carbons, the intensity between 40 and 80 ppm from the  $\text{C}_\alpha$  sites, and the intensity between about 10 and 40 ppm from other aliphatic carbons especially methyl groups. Although highly overlapped, the relative intensities of the signals provide a guide to the sensitivity in  $^{13}\text{C}$ -detected solid-state NMR experiments. Notably, the lowest signal-to-noise ratio is observed for the sample with the highest degree of  $^{13}\text{C}$  labeling (Fig. 5D) because of the broadening effects of the homonuclear  $^{13}\text{C}$  dipolar couplings.

The one-dimensional solution  $^{13}\text{C}$  NMR spectra of the fractionally  $^{13}\text{C}$  labeled samples have peak intensities that are homogeneously scaled according to the  $^{13}\text{C}$  dilution ratio for all carbon

regions compared to 100% uniform  $^{13}\text{C}$  labeling (Column B in Fig. 5D–F). Many signals of carbonyl, aromatic, and aliphatic carbons are resolved in the  $[45\%^{13}\text{C}]$  labeled protein, however, at 25% labeling the majority of signals are close to the level of noise under comparable experimental conditions, showing the direct effect of isotopic dilution when homonuclear dipolar couplings are not a factor. The  $^{13}\text{C}$  NMR spectra in Column B of Fig. 5 indicate the differences in the labeling from media containing  $[2-^{13}\text{C}]$ -glucose,  $[2-^{13}\text{C}]$ -glycerol, and  $[1,3-^{13}\text{C}]$ -glycerol. Compared to uniform labeling, the  $[2-^{13}\text{C}]$ -glycerol sample has reduced intensity in the aliphatic, aromatic, and carbonyl regions of the spectrum, whereas the  $[1,3-^{13}\text{C}]$ -glycerol sample shows a complementary labeling pattern with diminished intensity in the  $\alpha$ -carbon resonance region. The overall level of isotopic labeling in the  $[2-^{13}\text{C}]$ -glycerol and  $[2-^{13}\text{C}]$ -glucose samples is similar, however, the spectral patterns are different, for example the strong aromatic resonances in the spectrum of  $[2-^{13}\text{C}]$ -glycerol are missing in the spectrum of the  $[2-^{13}\text{C}]$ -glucose sample.

The extent of labeling of the  $\text{C}_\alpha$ ,  $\text{C}_\beta$ , and  $\text{C}_\gamma$  sites differ only slightly from the expected average value for the various amino acids as indicated by the data in Fig. 6A. In contrast to the even distributions of the random fractional labeling, the samples labeled by incorporation of  $[2-^{13}\text{C}]$ -glucose have quite different levels of  $^{13}\text{C}$  enrichment in different sites (Fig. 6B and C).

In the case of  $[2-^{13}\text{C}]$ -glucose labeling in *P. aeruginosa*, at least 14 amino acids have isolated  $^{13}\text{C}_\alpha$  labels. The enrichment ratio between the  $[2-^{13}\text{C}]$ -glucose and a uniformly  $^{13}\text{C}$  labeled sample at the  $\text{C}_\alpha$  position of glycine, leucine, glutamine, arginine, serine, and tyrosine is less than 20%. Glycine, serine, and tyrosine are highly enriched in *E. coli* [3], however, due to the Entner–Doudoroff metabolic pathway in *P. aeruginosa* these amino acids are omitted in the  $^{13}\text{C}$  labeling [6]. With the exception of glycine, leucine, glutamine, arginine, serine, and tyrosine, in total 14 of 20 amino acids in *P. aeruginosa*, and in *E. coli* all amino acids except from leucine provide isolated  $^{13}\text{C}_\alpha$  labels (Fig. 7) For  $[2-^{13}\text{C}]$ -glycerol as labeling precursor in *P. aeruginosa* only leucine, glutamine, and arginine are not enriched above 20% at the  $\text{C}_\alpha$  site. Isoleucine and valine have significant  $^{13}\text{C}$  enrichment at the adjacent  $\text{C}_\beta$ , and will be affected by  $^{13}\text{C}$ – $^{13}\text{C}$  dipolar coupling. A set of 15 of the 20 amino acids in proteins obtained from *P. aeruginosa* grown on  $[2-^{13}\text{C}]$ -glycerol-containing media is found to be suitable for  $^{13}\text{C}$  solid-state NMR experiments (Fig. 4C).

The effects of tailoring the  $^{13}\text{C}$  labeling are readily observed in  $^{13}\text{C}$  NMR spectra. As noted above, because of the strong influence of the  $^{13}\text{C}$ – $^{13}\text{C}$  homonuclear dipole–dipole couplings there is not

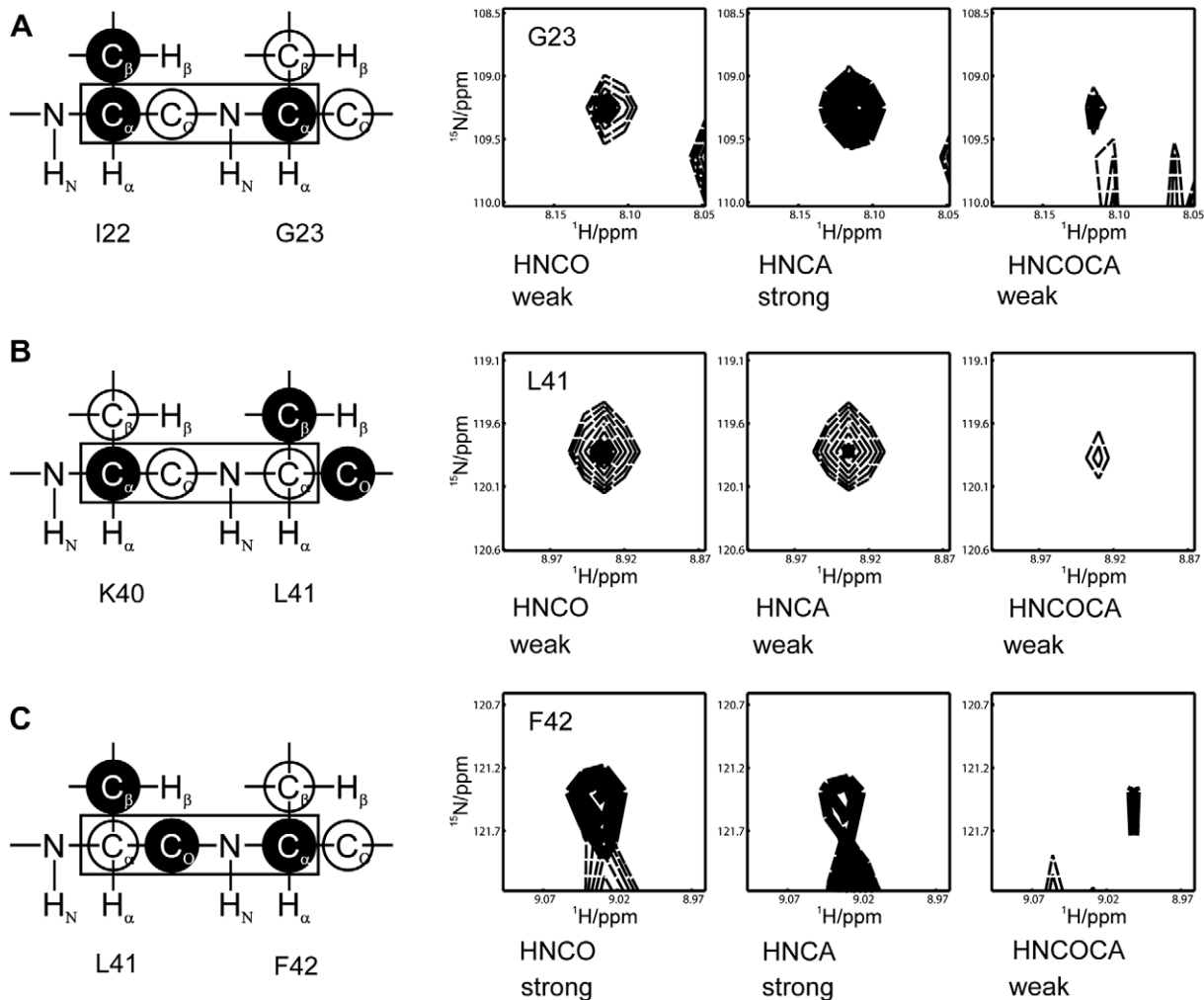


**Fig. 3.** Analysis of  $^{13}\text{C}$  labeling using  $^{13}\text{C}$ -edited two-dimensional  $^1\text{H}/^{15}\text{N}$  correlation spectra. Left column, topology of  $^{13}\text{C}$  labeling (black) from a sample obtained from bacteria grown on  $[2-^{13}\text{C}]$ -glucose-containing media. (A) Isoleucine 22 linked to glycine 23. (B) Lysine 40 linked to leucine 41. (C) Leucine 41 linked to phenylalanine 42. Right column, experimental two-dimensional  $^1\text{H}/^{15}\text{N}$  projections of three-dimensional HNCO, HNCA, and HNCOCA protein backbone spectra. Spectra from the sample obtained by growth on  $[2-^{13}\text{C}]$ -glucose-containing media (thick lines) is compared with a 25% uniformly  $^{13}\text{C}$  labeled sample (thin dashed lines).

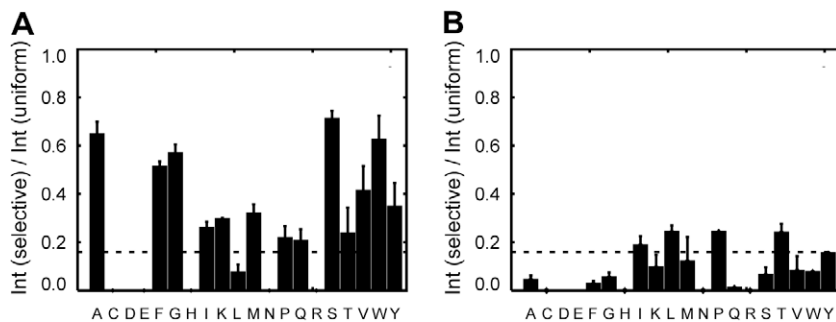


**Fig. 4.** Experimentally observed  $^{13}\text{C}$  labeling of fd coat protein obtained from *E. coli* grown on  $[2-^{13}\text{C}]$ -glucose-containing media as measured from intensities in  $^1\text{H}-^{13}\text{C}$  projections of HNCO and HNCA spectra. (A)  $\text{C}_\alpha$  sites. (B)  $\text{C}_0$  sites. The dashed lines mark 18% labeling, which is the level used to designate those sites that are likely to provide observable signals in solid-state NMR experiments.

a simple relationship between the extent or type of  $^{13}\text{C}$  labeling and the resolution and sensitivity. The spectra of the random fractionally labeled samples have higher signal-to-noise ratios than that of a comparable uniformly  $^{13}\text{C}$  labeled sample. The metabolic  $\text{C}_\alpha$  labeling schemes based on  $[2-^{13}\text{C}]$ -glucose and  $[2-^{13}\text{C}]$ -glycerol show strong signals in the one-dimensional solid-state NMR spectra, compared to the broad, poorly resolved spectra from

samples with uniform 100%  $^{13}\text{C}$  labeling. In contrast to the random fractionally labeled samples, the samples labeled with  $[2-^{13}\text{C}]$ -glucose and  $[2-^{13}\text{C}]$ -glycerol have relatively high overall labeling of the  $\alpha$ -carbons and significantly lower levels of labeling of carbonyl and aliphatic side chain carbons. The  $[1,3-^{13}\text{C}]$ -glycerol sample has more extensive labeling of carbonyl and side chain methyl carbons, and the spectra have better resolution in these regions.

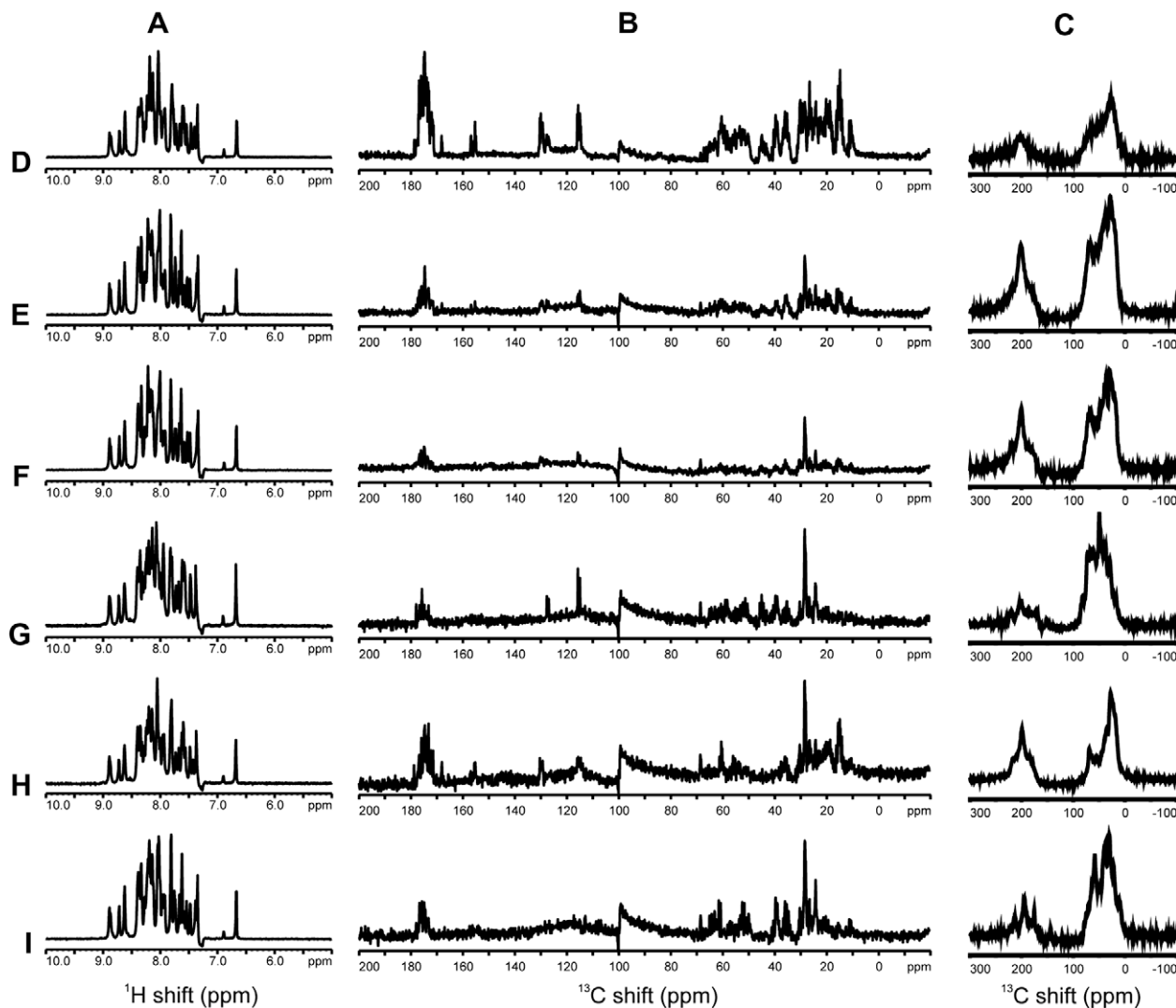


**Fig. 5.** Comparison of NMR spectra of 100% uniformly  $^{15}\text{N}$  labeled and fractional uniformly  $^{13}\text{C}$  labeled samples of Pf1 coat protein obtained from *P. aeruginosa*. Column A,  $^{15}\text{N}$ -edited  $^1\text{H}$  solution NMR spectra of the protein in micelles. Column B, direct-detected solution  $^{13}\text{C}$  NMR spectra obtained by direct excitation of the protein in micelles. Column C,  $^{13}\text{C}$ -detected cross-polarization solid-state NMR spectra obtained with both  $\{^1\text{H}\}$  and  $\{^{15}\text{N}\}$  decoupling during acquisition. (D) One-hundred percent uniformly  $^{13}\text{C}$  labeled. (E) Forty-five percent uniformly  $^{13}\text{C}$  labeled. (F) Twenty-five percent uniformly  $^{13}\text{C}$  labeled. (G) From growth on  $[2\text{-}^{13}\text{C}]$ -glycerol-containing media. (H) From growth on  $[1,3\text{-}^{13}\text{C}]$ -glycerol-containing media. (I) From growth on  $[2\text{-}^{13}\text{C}]$ -glucose-containing media.

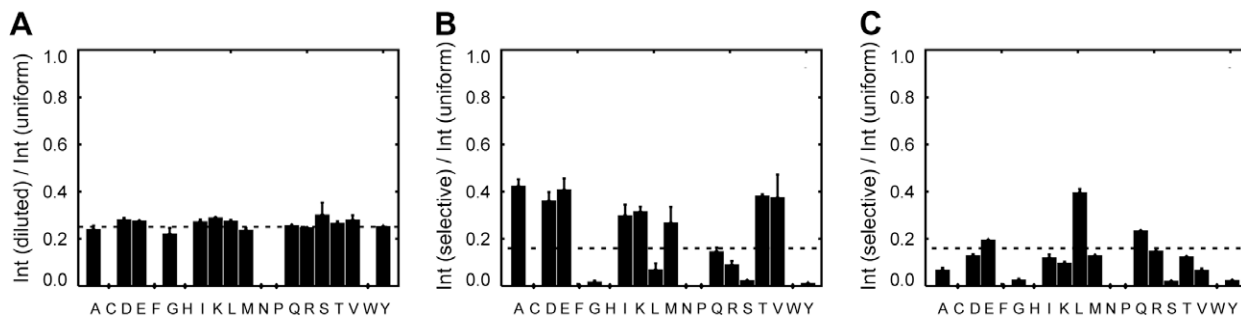


**Fig. 6.** Experimentally observed  $^{13}\text{C}$  labeling at the Pf1 coat protein obtained from *P. aeruginosa* grown on three different types of  $^{13}\text{C}$ -containing media. The intensity ratios are measured from  $^1\text{H}, ^{13}\text{C}$ -projections of HNC0 and HNCA spectra compared to those from a 100% uniformly  $^{13}\text{C}$  sample. (A)  $\text{C}_\alpha$  sites of a 25% uniformly  $^{13}\text{C}$  labeled protein sample. The dashed line marks 25% labeling. (B)  $\text{C}_\alpha$  sites of a protein sample obtained from growth on  $[2\text{-}^{13}\text{C}]$ -glucose-containing media. (C)  $\text{C}_\beta$  sites of a protein sample obtained from growth on  $[2\text{-}^{13}\text{C}]$ -glucose-containing media. In (B and C), the dashed lines mark 18% labeling, as in Fig. 4.

The effects of tailoring  $^{13}\text{C}$  labeling can also be observed in  $^{15}\text{N}$  NMR spectra. Although the effects are more subtle than those in the directly detected  $^{13}\text{C}$  NMR spectra, they are apparent in comparisons of  $^{15}\text{N}$  NMR spectra obtained with and without heteronu-

clear  $^{13}\text{C}$  decoupling. This is illustrated with the spectra in Fig. 8. The spectra in the left column are all very similar; since they were obtained with  $^1\text{H}$  and  $^{13}\text{C}$  decoupling, the effects of the  $^{13}\text{C}\text{-}^{15}\text{N}$  dipolar couplings are not seen. In contrast, the spectra in the right



	A	C	D	E	F	G	H	I	K	L	M	N	P	Q	R	S	T	V	W	Y
<b>A</b>	*	*	*	*	*	*	*	*	*	*	*	*	*	*	*	*	*	*	*	*
$C_{\alpha}$	+	+	+	+	+	+	+	+	+	-	+	+	+	+	+	+	+	+	+	+
$C_{\beta}$	-	-	-	-	-	-	-	-	-	-	-	-	-	-	-	-	-	-	-	-
$C_{O}$	-	-	-	-	-	-	-	+/-	-	+/-	-	-	+/-	-	-	-	+/-	-	-	-
Isolated	+	+	+	+	+	+	+	+	+	-	+	+	+	+	+	+	+	+	+	+
<b>B</b>	*	*	*	*	*	*	*	*	*	*	*	*	*	*	*	*	*	*	*	*
$C_{\alpha}$	+	+	+	+	-	+	+	+	-	+	+	+	+/-	-	-	+	+	+	-	-
$C_{\beta}$	-	-	-	-	-	-	+/-	-	-	-	-	-	-	-	-	-	-	+/-	-	-
$C_{O}$	-	-	-	+/-	-	-	-	-	+	-	-	-	+/-	-	-	-	-	-	-	-
Isolated	+	+	+	+	-	+	+	+	-	+	+	+	-	-	-	-	+	+	+	-
<b>C</b>	*	*	*	*	*	*	*	*	*	*	*	*	*	*	*	*	*	*	*	*
$C_{\alpha}$	+	+	+	+	+	+	+	+	+	-	+	+	+	-	-	+	+	+	+	+
$C_{\beta}$	-	-	-	-	-	-	-	+	-	-	-	-	-	-	-	-	-	+	-	-
$C_{O}$	-	-	-	+/-	-	-	-	-	+	-	-	-	+/-	-	-	-	-	-	-	-
Isolated	+	+	+	+	+	+	+	-	+	-	+	+	-	-	+	+	-	+	-	+

**Fig. 7.** Amino acids with isolated  $C_{\alpha}$  sites in the polypeptide backbone with >18% labeling. The amino acids present in Pf1 coat protein are marked by asterisks; for those amino acids that do not occur in the protein, the labeling anticipated from the Entner–Doudoroff pathway is included for completeness. The presence or absence of significant  $^{13}\text{C}$  labeling in the  $C_{\alpha}$ ,  $C_{\beta}$ , and  $C_{O}$  sites of the specified amino acids is designated in the horizontal rows. If the labeling at a  $C_{\alpha}$  site is >18% and the labeling at the bonded  $C_{\beta}$  and  $C_{O}$  sites is <18%, then the  $C_{\alpha}$  site is marked as + isolated. A few marginal cases are marked +/-.

(A) Protein obtained from *E. coli* grown on media containing [2- $^{13}\text{C}$ ]-glucose. (B) Protein obtained from *P. aeruginosa* grown on media containing [2- $^{13}\text{C}$ ]-glucose. (C) Protein obtained from *P. aeruginosa* grown on media containing [2- $^{13}\text{C}$ ]-glycerol.

column were obtained on the same samples with only  $^1\text{H}$  decoupling. The broadening effects of nearby  $^{13}\text{C}$  labeled sites on the  $^{15}\text{N}$  amide backbone resonances can be observed to vary among the labeling schemes.

Two-dimensional  $^1\text{H}$ – $^{13}\text{C}$  PISEMA spectra of aligned bacteriophage samples prepared with the various  $^{13}\text{C}$  labeling schemes are compared in Fig. 9. In the 100% uniformly  $^{13}\text{C}$  labeled sample, the strong network of  $^{13}\text{C}$ – $^{13}\text{C}$  homonuclear couplings at all sites interferes with the experiment and, with the exception of the methyl carbon region between 10 and 40 ppm, there is essentially no intensity observable in the displayed spectral region, which encompasses all of the aliphatic carbon sites in the protein. In contrast, all of the samples with tailored  $^{13}\text{C}$  labeling yield resolved spectra. The spectra from Pf1 coat protein obtained from bacteria grown on media containing [2- $^{13}\text{C}$ ]-glycerol or [1,3- $^{13}\text{C}$ ]-glycerol are complementary, due to the specific metabolic labeling pattern of the glycerol precursors. There is notably more intensity from aliphatic side chain carbons in the spectrum obtained from the [1,3- $^{13}\text{C}$ ]-glycerol due to its labeling pattern. Although the total amount of  $^{13}\text{C}$  in the protein is reduced, there is a net gain in signal-to-noise ratio in all of the one-dimensional spectra. Although less than half of the carbon sites are labeled in the case of [45%- $^{13}\text{C}$ ] phage, the observed signal-to-noise ratio is about twice that observed for the 100% labeled phage. As expected, the signal-to-noise ratio decreases with decreasing  $^{13}\text{C}$  content, however, even [15%- $^{13}\text{C}$ ] phage gives spectra with better signal-to-noise ratios than those from a 100% uniformly  $^{13}\text{C}$  labeled sample. The gain in signal-to-noise ratio is greater in the case of proteins obtained from media containing specifically labeled glucose or glycerol.

The analysis of the two-dimensional solid-state NMR spectra reveals different line shape behavior for the  $^{13}\text{C}$  chemical shift and the  $^1\text{H}$ – $^{13}\text{C}$  dipolar coupling dimensions. For all of the samples the full width at half height is approximately 250–300 Hz in the  $^{13}\text{C}$  chemical shift dimension, except with [45%- $^{13}\text{C}$ ] labeling where the samples have somewhat broader lines of 400 Hz. For the  $^1\text{H}$ – $^{13}\text{C}$  dipolar coupling dimension, the different dilutions of the  $^{13}\text{C}$  affect the line width of the two-dimensional spectra. For the spectra of the random fractional labeled samples the full width at half height decreases with increasing  $^{13}\text{C}$  dilution from 1300 Hz for [45%- $^{13}\text{C}$ ] phage to 700 Hz for [15%- $^{13}\text{C}$ ] phage. For the metabolically tailored  $^{13}\text{C}$  labeling schemes the full width at half height of the two-dimensional spectra is between 1350 and 900 Hz, with the [1,3- $^{13}\text{C}$ ]-glycerol and [2- $^{13}\text{C}$ ]-glucose labeled samples providing spectra with somewhat better resolution than those labeled with [2- $^{13}\text{C}$ ]-glycerol.

Although there is a reduction in signal-to-noise with decreasing  $^{12}\text{C}$  to  $^{13}\text{C}$  isotope ratio, this is compensated by improvement in the line shape in the  $^1\text{H}$ – $^{13}\text{C}$  dipolar coupling dimension whereas the  $^{13}\text{C}$  chemical shift dimension is hardly affected (Fig. 10). For the two different  $C_{\alpha}$  labeling precursors, [2- $^{13}\text{C}$ ]-glycerol and [2- $^{13}\text{C}$ ]-glucose, the later shows a better line shape in both dimensions of the two-dimensional spectra. The [1,3- $^{13}\text{C}$ ]-glycerol sample yields slightly better line shapes for the  $C_{\alpha}$  sites.

### 3. Discussion

Uniform isotopic labeling of proteins has been an integral part of the experimental design from the beginning of the field [11,18], and 100% uniform labeling with  $^{13}\text{C}$  and  $^{15}\text{N}$  is widely used in triple-resonance solution NMR experiments as well as MAS solid-state NMR experiments. Because of the natural isolation of nitrogen sites in proteins, there is no need to vary the extent of  $^{15}\text{N}$  labeling because of through-space or through-bond couplings. However, all carbons are bonded to at least one other carbon and in most cases two other carbons, resulting in dense networks of homonuclear scalar and/or dipole–dipole couplings that can interfere with both solution NMR and solid-state NMR experiments. The two basic strategies for  $^{13}\text{C}$  labeling that are evaluated in the context of aligned-sample solid-state NMR experiments with the data in Figs. 8 and 9 were previously used for solution NMR and magic angle spinning solid-state NMR. In solution NMR, the preparation of protein samples that were uniformly fractionally  $^{13}\text{C}$  labeled enabled  $J$  couplings to be used to assist in making resonance assignments [19] and to simplify relaxation pathways [20]. Biosynthetic incorporation of specifically  $^{13}\text{C}$  labeled metabolic precursors, including glycerol [21], glucose [22], and pyruvate [23], were also used to facilitate  $^{13}\text{C}$  relaxation studies and triple-resonance experiments solution NMR. Increased resolution in magic angle spinning solid-state NMR experiments has resulted primarily from the use of samples with complementary labeling patterns obtained from growth on media containing [1- $^{13}\text{C}$ ]-glycerol and [2,3- $^{13}\text{C}$ ]-glycerol [13–15].

The tailored labeling from the labeled glycerol improves the resolution that is possible with magic angle spinning of 100% uniformly  $^{13}\text{C}$  labeled samples. In contrast, in aligned-sample solid-state NMR, in order to obtain high-resolution spectra and realize the sensitivity gains feasible with  $^{13}\text{C}$  detection, the homonuclear dipole–dipole couplings have to be dealt with either by multiple-pulse homonuclear decoupling or isotopic labeling. As described here, an approach applicable to proteins obtained by expression in bacteria is to tailor the  $^{13}\text{C}$  labeling to label sites of interest, for example the  $\alpha$ -carbons, while adjacent carbon sites are unlabeled. In this continuation of our development of this approach, several complementary labeling schemes were tested for two dif-

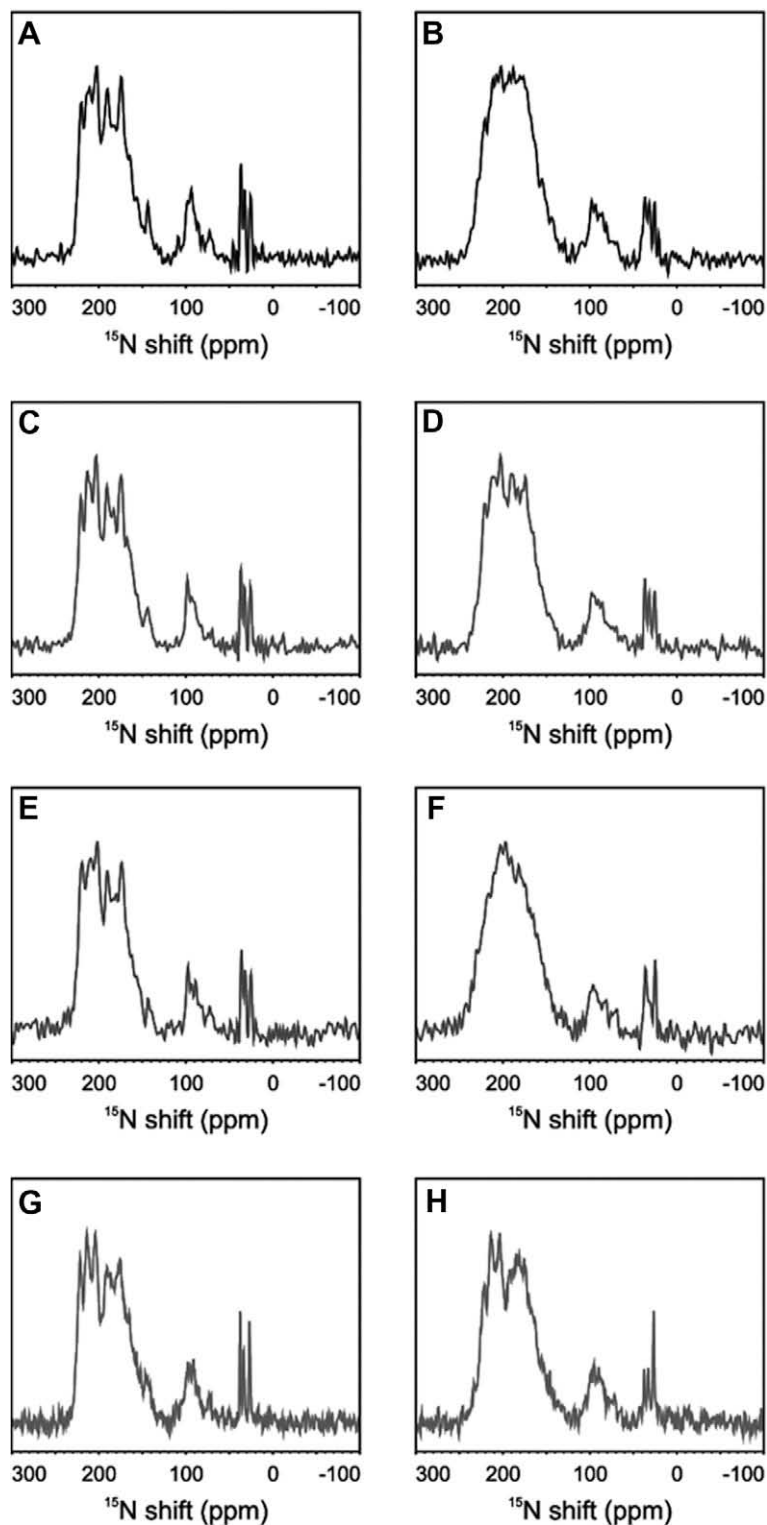


**Fig. 8.** Comparison of one-dimensional solid-state  $^{15}\text{N}$  NMR spectra of 100% uniformly  $^{15}\text{N}$  labeled and fractional uniformly  $^{13}\text{C}$  labeled samples of Pf1 coat protein obtained from *P. aeruginosa*. (A, C, E, and G) Obtained with both  $^1\text{H}$  and  $^{13}\text{C}$  decoupling. (B, D, F, and H) Obtained with only  $^1\text{H}$  decoupling. (A and B) Forty-five percent uniformly  $^{13}\text{C}$  labeled. (C and D) Twenty-five percent uniformly  $^{13}\text{C}$  labeled. (E and F) Protein obtained from bacteria grown on  $[1,3\text{-}^{13}\text{C}]$ -glycerol-containing media. (G and H) Protein obtained from bacteria grown on  $[1,2\text{-}^{13}\text{C}]$ -glucose-containing media.

ferent bacteria. The  $^{13}\text{C}$  dilution from random fractional labeling media had predictable outcomes for both tested expression systems. However, the implementation of metabolic precursors for labeling depends on the organism's specific metabolic pathways, and requires experimental verification. The choice of labeling strat-

egy is an integral part of the experimental design, which contrasts with the situation for most solution NMR and magic angle spinning solid-state NMR studies that can be accomplished with only one or a few labeled sample prepared according to the previously demonstrated labeling schemes.

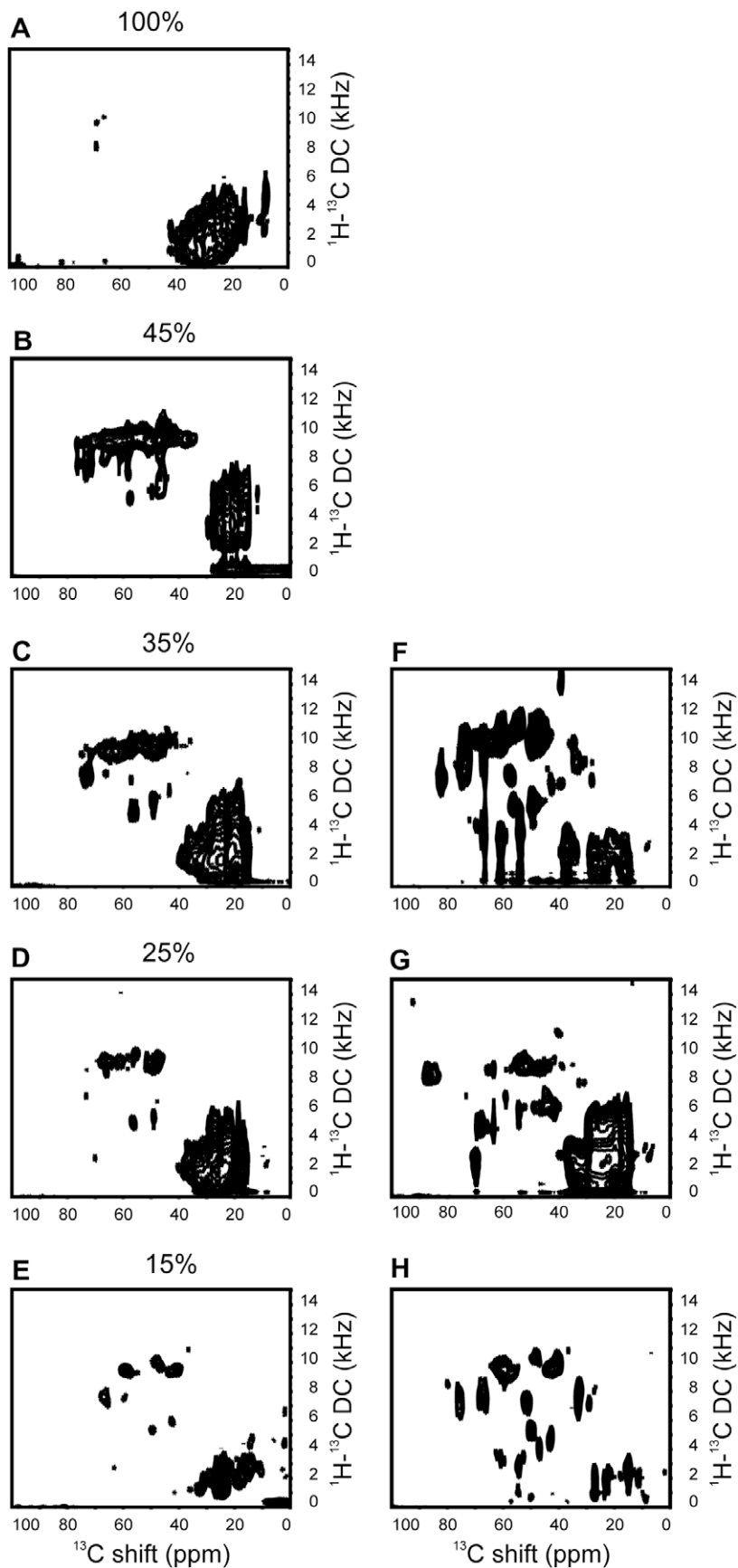


**Fig. 9.** Comparison of two-dimensional  $^1\text{H}$ - $^{13}\text{C}$  PISEMA spectra of aligned Pf1 bacteriophage samples. (A) One-hundred percent uniformly  $^{13}\text{C}$  labeled. (B–E) Fractional uniformly  $^{13}\text{C}$  labeled at the indicated percentages. (F) From bacteria grown on  $[2\text{-}^{13}\text{C}]$ -glycerol-containing media. (G) From bacteria grown on  $[1,3\text{-}^{13}\text{C}]$ -glycerol-containing media. (H) From bacteria grown on  $[2\text{-}^{13}\text{C}]$ -glucose-containing media.



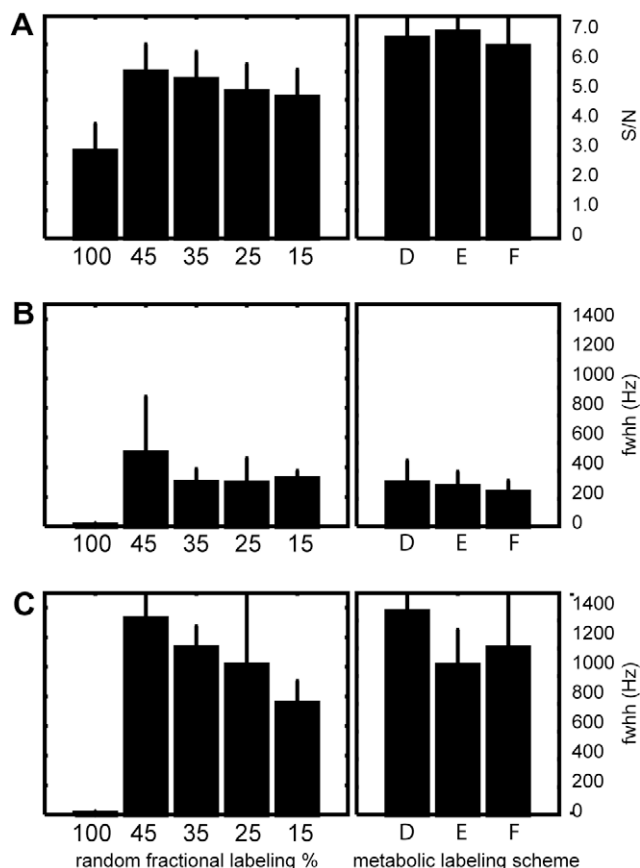


**Fig. 10.** Comparison of single-to-noise ratios and resonance linewidths in the  $^1\text{H}$ - $^{13}\text{C}$  PISEMA spectra of aligned Pf1 bacteriophage. The error bars represent the estimated uncertainty in the measurements made on the experimental spectra in Fig. 9. (A) Signal-to-noise ratios of the one-dimensional solid-state NMR spectra. (B) Full width at half height of the  $^{13}\text{C}$  chemical shift dimension. (C) Full width at half height of  $^1\text{H}$ - $^{13}\text{C}$  dipolar coupling dimension. Left panels, the percentages listed on the bottom correspond to the extent of fractional uniform  $^{13}\text{C}$  labeling. Right panels,  $^{13}\text{C}$  labeling from bacteria grown in media containing D,  $[2\text{-}^{13}\text{C}]$ -glycerol. E,  $[1,3\text{-}^{13}\text{C}]$ -glycerol. F,  $[2\text{-}^{13}\text{C}]$ -glucose.

For aligned-sample solid-state NMR of proteins, the optimal percentage for uniform fractional  $^{13}\text{C}$  labeling is between 25% and 35%. Specifically labeled glycerol and glucose can be used at the carbon sources to tailor the isotopic labeling, and the choice depends on the resonances of interest for a particular study. For investigations of the protein backbone,  $[2\text{-}^{13}\text{C}]$ -glucose was found to be most effective. In the case of *P. aeruginosa* there are 14 of the 20 amino acids with isolated  $\text{C}_\alpha$  position in the protein backbone and for *E. coli*. Nineteen amino acids have  $^{13}\text{C}_\alpha$  sites.

## 4. Methods

### 4.1. Sample preparation

The 100% uniformly  $^{13}\text{C}$  and  $^{15}\text{N}$  labeled samples were obtained in the conventional way by using a minimal salts media with  $^{15}\text{N}$  labeled ammonium sulfate and  $^{13}\text{C}_6$  labeled glucose as the sole nitrogen and carbon sources. Uniform fractional  $^{13}\text{C}$  labeling was performed by growing bacteria on standard BioExpress Cell Growth Media prepared with the stated percentages of  $^{13}\text{C}$ . The metabolically  $^{13}\text{C}$  labeled samples were obtained by supplementing the using  $[2\text{-}^{13}\text{C}]$ -glycerol,  $[2\text{-}^{13}\text{C}]$ -glycerol,  $[1,3\text{-}^{13}\text{C}]$ -glycerol, or as the sole carbon source. All of the isotopically labeled compounds and media described in this article are from Cambridge Isotope Laboratories ([www.isotope.com](http://www.isotope.com)).

The 50 mg/ml solutions of aligned bacteriophage particles were prepared as described previously [24]. The coat proteins subunits were separated from the phage particles and solubilized in SDS for the solution NMR analysis [25].

### 4.2. NMR spectroscopy

The solid-state NMR experiments were performed on a Varian Inova spectrometer with  $^1\text{H}$ ,  $^{13}\text{C}$ , and  $^{15}\text{N}$  frequencies of 500.125 MHz, 125.76 MHz, and 50.68 MHz, respectively. A home-built triple resonance probe with a single 5 mm solenoid coil was used and the RF power levels were adjusted to generated 50 kHz RF fields on all three channels. PISEMA was utilized for the separated local field experiments because its cycle time was short enough to accommodate the large frequencies of  $^1\text{H}$ - $^{13}\text{C}$  dipolar couplings. The  $^1\text{H}$  carrier frequency was set to the resonance of water at 4.7 ppm; the  $^{13}\text{C}$  and  $^{15}\text{N}$  carrier frequencies were set to 100 ppm on their respective scales. Solid samples of adamantane and ammonium sulfate served as external chemical shift references for  $^{13}\text{C}$  and  $^{15}\text{N}$ , respectively. The two-dimensional solid-state NMR spectra were acquired with 64 points in  $t_1$  and 512 complex points in  $t_2$ . The experimental data were zero filled in  $t_1$  to 2K and in  $t_2$  to 4K data points and multiplied by a sine bell window function before Fourier transformation in each dimension. The recycle delay was 6 s.

The solution NMR experiments were performed on a Bruker Avance 800 MHz spectrometer with  $^1\text{H}$ ,  $^{13}\text{C}$ , and  $^{15}\text{N}$  frequencies of 800.034 MHz, 201.203 MHz, and 81.076 MHz, respectively. For these experiments, the coat proteins of the bacteriophages were solubilized in SDS micelles at a concentration of 1 mM. Resonance assignments of  $\text{C}_\alpha$ ,  $\text{C}_\beta$ , or  $\text{C}_\gamma$  sites for the solution-state NMR spectra were obtained from three-dimensional HNCA, HNCB, and HNCO experiments on a 100% uniformly  $^{13}\text{C}$ ,  $^{15}\text{N}$  labeled sample. Resonance assignments of  $\text{H}_\alpha$  for the  $^1\text{H}$ ,  $^{13}\text{C}$ -HSQC spectra were obtained from a three-dimensional  $^{15}\text{N}$ -edited NOESY-HSQC experiment with a mixing time of 120 ms.  $\text{C}_\beta$  and  $\text{C}_\gamma$  resonance measurements NMR spectra were obtained from three-dimensional HNCA, HNCB, and HNCO experiments.  $^{13}\text{C}$  chemical shift was referenced indirectly to the  $^1\text{H}$  chemical shift of DSS.

### Acknowledgments

We thank Christopher Grant, Chin Wu, and Xuemei Huang for helpful discussions and assistance with the instrumentation. This research was supported by grants from the National Institutes of Health, and utilized the Biomedical Technology Resource for NMR Molecular Imaging of Proteins, which is supported by Grant P41EB002031. F.V.F. was supported by an EMBO postdoctoral fellowship (ALTF 214-2007).

### References

- [1] S.J. Opella, F.M. Marassi, Structure determination of membrane proteins by NMR spectroscopy, *Chem. Rev.* 104 (2004) 3587–3606.
- [2] T.A. Cross, J.A. DiVerdi, S.J. Opella, Strategy for nitrogen NMR analysis of biopolymers, *J. Am. Chem. Soc.* 104 (1982) 1759–1761.
- [3] Z. Gu, S.J. Opella, Three-dimensional  $^{13}\text{C}$  Shift/ $^1\text{H}$ - $^{15}\text{N}$  Coupling/ $^{15}\text{N}$  Shift solid-state NMR correlation spectroscopy, *J. Magn. Reson.* 138 (1999) 193–198.
- [4] Z. Gu, S.J. Opella, Two- and three-dimensional  $^1\text{H}/^{13}\text{C}$  PISEMA experiments and their application to backbone and side chain sites of amino acids and peptides, *J. Magn. Reson.* 140 (1999) 340–346.
- [5] D.M. Schneider, R. Tycko, S.J. Opella, High-resolution solid-state triple nuclear magnetic resonance measurement of  $^{13}\text{C}$ - $^{15}\text{N}$  dipole-dipole couplings, *J. Magn. Reson.* 73 (1987) 568–573.
- [6] N. Sinha, C.V. Grant, K.S. Rotondi, L. Feduik-Rotondi, L.M. Gierasch, S.J. Opella, Peptides and the development of double- and triple-resonance solid-state NMR of aligned samples, *J. Peptide Res.* 65 (2005) 605–620.
- [7] N. Sinha, C.V. Grant, S.H. Park, J.M. Brown, S.J. Opella, Triple resonance experiments for aligned sample solid-state NMR of  $^{13}\text{C}$  and  $^{15}\text{N}$  labelled proteins, *J. Magn. Reson.* 186 (2007) 51–64.

- [8] N. Sinha, F.V. Filipp, L. Jairam, S.H. Park, J. Bradley, S.J. Opella, Tailoring  $^{13}\text{C}$  labeling for triple-resonance solid-state NMR experiments on aligned samples of proteins, *Magn. Reson. Chem.* 45 (2007) S107–S115.
- [9] W.M. Tan, Z. Gu, A.C. Zeri, S.J. Opella, Solid state NMR triple-resonance backbone assignments in a protein, *J. Biomol. NMR* 13 (1999) 337–342.
- [10] Y. Ishii, R. Tycko, Multidimensional heteronuclear correlation spectroscopy of a uniformly  $^{15}\text{N}$ - and  $^{13}\text{C}$ -labelled peptide crystal: toward spectral resolution, assignment, and structure determination of oriented molecules in solid-state NMR, *J. Am. Chem. Soc.* 122 (2000) 1443–1455.
- [11] L.-Y. Lian, D.A. Middleton, Labeling approaches for protein structural studies by solution-state and solid-state NMR, *Prog. Nucl. Magn. Reson. Spectrosc.* 39 (2001) 171–190.
- [12] J.S. Waugh, L.M. Huber, U. Haeberlen, Approach to high-resolution NMR in solids, *Phys. Rev. Lett.* 20 (1968) 180–183.
- [13] M. Hong, K. Jakes, Selective and extensive  $^{13}\text{C}$  labeling of a membrane protein for solid-state NMR investigations, *J. Biomol. NMR* 14 (2001) 71–74.
- [14] F. Castellani, B. van Rossum, A. Diehl, M. Schubert, K. Rehbein, H. Oschkinat, Structure of a protein determined by solid-state magic-angle-spinning NMR spectroscopy, *Nature* 420 (2002) 98–102.
- [15] B.J. Wylie, C.M. Rienstra, Multidimensional solid state NMR of anisotropic interactions in peptides and proteins, *J. Chem. Phys.* 128 (2008) 052207.
- [16] A. Goldbourn, B.J. Gross, L.A. Day, A.E. McDermott, Filamentous phage studied by magic-angle spinning NMR: resonance assignment and secondary structure of the coat protein in Pf1, *J. Am. Chem. Soc.* 129 (2007) 2338–2344.
- [17] A. Goldbourn, L.A. Day, A.E. McDermott, Assignment of congested NMR spectra: carbonyl backbone enrichment via the Entner–Doudoroff pathway, *J. Magn. Reson.* 189 (2007) 157–165.
- [18] C.G. Hoogstraten, J.E. Johnson, Metabolic labeling: taking advantage of bacterial pathways to prepare spectroscopically useful isotope patterns in proteins and nucleic acids, *Concepts Magn. Reson. A* 32 (2008) 34–55.
- [19] B.H. Oh, W.M. Westler, P. Darba, J.L. Markley, Protein carbon-13 spin systems by a single two-dimensional nuclear magnetic resonance experiment, *Science* 240 (1988) 908–911.
- [20] R.A. Venters, T.L. Calderone, L.D. Spicer, C.A. Fierke, Uniform  $^{13}\text{C}$  isotope labeling of proteins with sodium acetate for NMR studies: application to human carbonic anhydrase II, *Biochemistry* 30 (1991) 4491–4494.
- [21] D.M. Lemaster, D.M. Kushaln, Dynamical mapping of *E. coli* thioredoxin via  $^{13}\text{C}$  NMR relaxation analysis, *J. Am. Chem. Soc.* 118 (1996) 9255–9264.
- [22] P. Lundstrom, K. Teilum, T. Carstensen, I. Bezonova, S. Wisner, D.F. Hansen, T.L. Religa, M. Akke, L.E. Kay, Fractional  $^{13}\text{C}$  enrichment of isolated carbons using  $[1-^{13}\text{C}]$ - or  $[2-^{13}\text{C}]$ -glucose facilitates the accurate measurement of dynamics at backbone Ca and side-chain methyl positions in proteins, *J. Biomol. NMR* 38 (2007) 199–212.
- [23] C. Guo, C. Geng, V. Tugarinov, Selective backbone labeling of proteins using  $[1,2-^{13}\text{C}]$ -pyruvate as carbon source, *J. Biomol. NMR* 44 (2009) 167–173.
- [24] D.S. Thiriot, A.A. Nevzorov, C.H. Wu, L. Zagayanskiy, S.J. Opella, Structure of the coat protein in Pf1 bacteriophage determined by solid-state NMR spectroscopy, *J. Mol. Biol.* 341 (2004) 869–879.
- [25] P.A. McDonnell, K. Shon, Y. Kim, S.J. Opella, fd Coat protein structure in membrane environments, *J. Mol. Biol.* 233 (1993) 447–463.